Influences of trisomy 21 on neural progenitor cells in the fetal human neocortex

by

Aya Tuma

A thesis submitted to the Department of Biological Sciences, University of Manitoba,

in partial fulfillment of the requirements for the course

BIOL 4100 (Honours Thesis)

for the degree of

Bachelor of Science (Honours)

© April 2026

Abstract

Trisomy 21 (T21), also known as Down syndrome, is the most common genetic cause of intellectual disability. The neocortex is the seat of higher-order cognitive functions, such that its altered fetal development may contribute to this phenotype. Neurodevelopment must be tightly regulated by signalling pathways to ensure proper neurogenesis and gliogenesis. The growth differentiation factor 15 (GDF15) pathway is of interest as peak GDF15 production coincides with peak basal progenitor proliferation in the developing neocortex. However, little is known about this pathway in fetal T21 neurodevelopment. This study aimed to identify the alterations in neocortex cytoarchitecture and the GDF15 pathway in the fetal T21 neocortex. Using human tissue, there was no significant difference in the abundance of SOX2-, SATB2-, and OLIG1-positive cells between euploid and T21 neocortices, collectively, but a potential reduction in SOX2-positive cells and increase in SATB2- and OLIG1-positive cells in T21 at PCW 13 relative to euploid PCW 12 was observed. The abundance of S100B-positive cells was significantly reduced, but expression of *OLIG1*, *OLIG2*, and *S100B* was significantly elevated in T21. There was no significant difference in the abundance of cells positive for and gene expression of GDF15 targets, DACH1 and GPC6, between euploid and T21 neocortices, but a potential reduction in these cells was observed in T21 at PCW 13 relative to euploid PCW 12. Gene expression of another GDF15 target, *SEMA5A,* was significantly elevated in T21 neocortices relative to euploid. These findings highlight the potential influence of the GDF15 pathway on neural progenitor cell dynamics and axon guidance in the fetal neocortex. While an expanded sample size is needed to determine the significance of these trends across different gestational ages, these results may serve to

expand our understanding of T21 and develop support programs for individuals with the syndrome.

Acknowledgements

I would like to extend my sincerest gratitude and thanks to my advisor, Dr. Lei Xing, for his unwavering guidance, feedback, and mentorship throughout my time in his lab. Thank you for helping me grow both personally and scientifically. I would also like to send my deepest appreciation to my committee members, Dr. Robert Beattie and Dr. Kevin Campbell, for their support throughout this project. Thank you both for sharing your valuable time and insight with me.

I would also like to thank the members of the Xing Lab who have shared their knowledge with me and made this experience even more valuable: Shirley Morris, Sounak Ray, Erica Wong, Kalan Azaransky, and Ho In Shin. You have all taught me so much about life, and I am excited to see what your futures hold.

Last, but certainly not least, I would like to extend my deepest and sincerest appreciation to my family, friends, and quiet supporters who have stood by me throughout this project. Mere words are not enough to express my gratitude to you all, but I hope you are aware of how integral your support has been in my journey. I hope I have made you proud. A special shoutout to my bird, Mango, who attempted to destroy my laptop numerous times over the past year, but never succeeded in stopping me from counting cells or writing.

Table of Contents

Abstract ..... **i**

Acknowledgements ..... **iii**

List of Tables ..... **vi**

List of Figures ..... **vii**

List of Abbreviations and Gene Names ..... **viii**

1. Introduction **1**

1.1. Study rationale 4

1.2. Objectives 5

1.3. Hypotheses and predictions 5

2. Materials and Methods **6**

2.1. Study design 6

2.1.1. Experimental approach 1: Immunofluorescence of neural progenitor cell abundance in euploid and T21 neocortices 6

2.1.2. Experimental approach 2: Gene expression in euploid and T21 neocortices 7

2.2. Fetal human neocortical tissue 8

2.3. Immunofluorescence and imaging 9

2.4. Quantification 11

2.5. RNA extraction and cDNA synthesis 12

2.6. Real-time quantitative polymerase chain reaction 12

2.7. Statistical analysis 14

3. Results 14

3.1. Elevated mRNA expression of chromosome 21 genes in trisomy 21 neocortices ..14

3.2. Neocortex cytoarchitecture and neural and glial progenitor cell abundance may be altered at post-conceptional week 13 16

3.3. Expression of growth differentiation factor 15 targets may be altered at post-conceptional week 13 24

3.4. Elevated expression of *SEMA5A*, a growth differentiation factor 15 target..... 25

4. Discussion 26

4.1. Elevated expression of glial genes on chromosome 21 may contribute to altered neural development 26

4.2. Early differentiation may contribute to potential reductions in NPC abundance 28

4.3. DACH1 and GPC6 may regulate early neurodevelopment and synaptogenesis 30

4.4. Elevated *SEMA5A* expression may alter axon guidance 31

5. Literature Cited 34

List of Tables

Table 1. Preservation method, developmental age, genotype, and sample sizes of fetal neocortical tissue samples used for data collection. **8**

Table 2. Primary and secondary antibodies used for immunofluorescence. **10**

Table 3. Primers used for RT-qPCR. **13**

List of Figures

Figure 1. Simplified pathway of NPC differentiation into neurons in the fetal neocortex..2

Figure 2. Relative mRNA expression levels of glial target genes in euploid and T21 fetal human neocortices. 15

Figure 3. Homeodomain-only protein X and SRY-box transcription factor 2 expression throughout the fetal euploid PCW 12 neocortex. 17

Figure 4. Homeodomain-only protein X and SRY-box transcription factor 2 expression in the fetal euploid and T21 oSVZ. 18

Figure 5. Dachshund family transcription factor 1 and phosphorylated vimentin expression in the fetal euploid and T21 neocortex and oSVZ..... 19

Figure 6. Glypican 6 and SATB homeobox 2 expression in the fetal euploid and T21 neocortex and oSVZ. 21

Figure 7. Oligodendrocyte transcription factor 1 and S100 calcium binding protein B expression in the fetal euploid and T21 neocortex and oSVZ. 23

Figure 8. Relative mRNA expression levels of GDF15 target genes in euploid and T21 fetal human neocortices. 25

List of Abbreviations and Gene Names

ACTB	Beta-actin
bRG	Basal radial glia
cDNA	Complementary DNA
DACH1	Dachshund family transcription factor 1
DAPI	4',6-diamidino-2-phenylindole
GAPDH	Glyceraldehyde-3-phosphate dehydrogenase
GDF15	Growth differentiation factor 15
GFRAL	Glial-cell derived neurotrophic factor family receptor alpha-like
GPC6	Glypican 6
HOPX	Homeodomain-only protein X
i/oSVZ	Inner/outer subventricular zone
NPC	Neural progenitor cell
OLIG1	Oligodendrocyte transcription factor 1
OLIG2	Oligodendrocyte transcription factor 2
PCW	Post-conceptional week
PVIM	Phosphorylated vimentin
RT-qPCR	Real-time quantitative polymerase chain reaction
S100B	S100 calcium-binding protein B
SATB2	SATB homeobox 2
SEMA5A	Semaphorin 5A
SHROOM3	Shroom family member 3
SOX2	SRY-box transcription factor 2
T21	Trisomy 21
VZ	Ventricular zone

1. Introduction

The neocortex is the largest and outermost layer of the cerebral cortex, and is a hallmark of mammalian evolution due to its significant expansion in the primate brain (especially in humans, *Homo sapiens*), and its roles in higher-order thinking and executive functioning[1,2]. The mature neocortex is comprised of six layers of specialized neurons that form connections among themselves and with other cerebral structures, with supportive glial cells dispersed throughout[1–4]. In humans, this intricate structure begins to form during early fetal development, at post-conceptional week (PCW) 7, through the processes of neurogenesis and gliogenesis[3–5].

Neurogenesis relies on various neural progenitor cells (NPCs) to give rise to neurons in the developing neocortex[1,2]. Briefly, the immature neocortex is divided into distinct cortical zones that differ in the cell types present and their organization – from the ventricles at the apical surface of the neocortex to the pia mater of the meninges at its basal lamina, these zones are the ventricular zone (VZ), inner and outer subventricular (iSVZ, oSVZ), intermediate zone, and cortical plate. Neurogenesis begins with the neuroepithelial cells of the embryonic neural tube. These cells give rise to the first cells of the fetal neocortex: apical radial glia, or basal progenitors – namely, the basal radial glia (bRG) and basal intermediate progenitors. Apical radial glia reside in the VZ, with their bipolar processes contacting the ventricle and basal lamina, while bRG reside primarily in the oSVZ, lack contact with the ventricles, but maintain a unipolar process contacting the basal lamina in the fetal human neocortex. Basal intermediate progenitors reside throughout the iSVZ and oSVZ, and are multipolar, lacking contact with the ventricular surface and basal lamina. Apical radial glia may differentiate to give rise to bRG, basal

intermediate progenitors, or apical intermediate progenitors residing in the VZ and only contacting the ventricle. These three classes of NPCs may give rise to other progenitor cells, or differentiate to form the first neurons of the developing neocortex (Fig. 1).

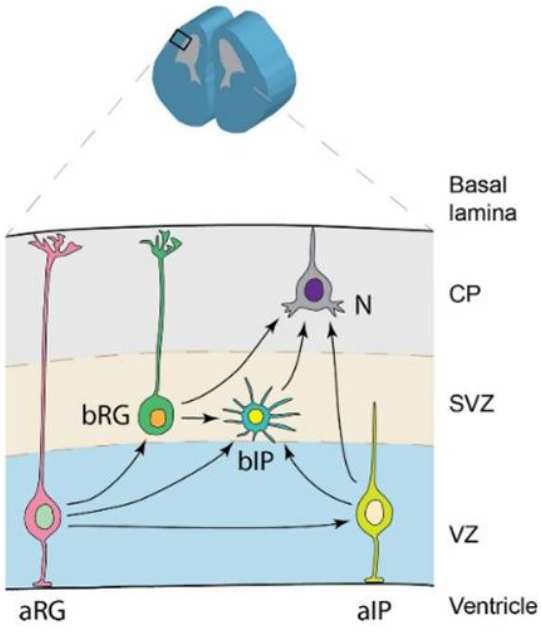

Figure 1. Simplified pathway of NPC differentiation into neurons in the fetal neocortex. aRG: apical radial glia; bRG: basal radial glia; aIP: apical intermediate progenitor; bIP: basal intermediate progenitor; N: neuron; VZ: ventricular zone; SVZ: subventricular zone; CP: cortical plate. Adapted from Xing et al. 2021[2].

While bRG may differentiate to form neurons, they may also transition from a neurogenic fate to a gliogenic fate in mid-gestation to give rise to macroglia – namely, astrocytes and oligodendrocytes – through gliogenesis[6,7]. It has been postulated that bRG give rise to pre-oligodendrocyte precursor cells, which populate the oSVZ at PCW 14, and differentiate to form oligodendrocyte precursor cells, which may give rise to immature oligodendrocytes or astrocytes[4,8,9]. Similarly, apical radial glia and bRG have been

postulated to give rise to astrocyte precursor cells residing in the oSVZ, which give rise to the protoplasmic astrocytes involved in forming the blood-brain barrier[3,4,7]. Regardless of the pathway taken by bRG to give rise to astrocytes and oligodendrocytes, the complexity of the neurogenic-gliogenic transition of bRG necessitates precise regulation.

A regulatory pathway of interest in fetal neurodevelopment is the growth differentiation factor 15 (GDF15) pathway. GDF15 is an inhibitory cytokine belonging to the transforming growth factor-beta superfamily[10]. Primarily produced in the placenta, GDF15 acts through binding to its receptor, glial-cell derived neurotrophic factor family receptor alpha-like (GFRAL), which is primarily localized to the hindbrain[10]. The effects of GDF15 are pleiotropic; GDF15 is associated with appetite regulation, cellular stress (e.g., cardiac failure), and low levels of this placental factor in pregnancy have been linked to preeclampsia and miscarriage[10,11]. Notably, *Gdf15* knock-out embryonic mice exhibit reduced NPC proliferation, highlighting the role of GDF15 in neurodevelopment[12]. In human embryonic development, GDF15 levels peak at PCW 9 to PCW 11, coinciding with peak basal progenitor proliferation; this association highlights the potential role of GDF15 in neocortical development[13]. Single-nucleus RNA sequencing of human NPCs has identified various potential downstream targets of GDF15, including glypican 6 (*GPC6*), dachshund family transcription factor 1 (*DACH1*), shroom family member 3 (*SHROOM3*), and semaphorin 5A (*SEMA5A*). Expression of the latter three genes also appears to peak between PCW 9 to PCW 11, while *GPC6* appears to peak at PCW15, further emphasizing the potential role of this pathway in embryonic neurodevelopment[13].

Little is known regarding the GDF15 pathway in the context of neurodevelopmental disorders. Such is the case for trisomy 21 (T21), colloquially known as Down syndrome. T21 is a genetic disorder caused by the complete or partial duplication of human chromosome 21 through meiotic non-disjunction or the inheritance of a Robertsonian translocation of human chromosome 21 onto chromosomes 14, 21, or 22 from a balanced carrier parent[14–16]. Individuals with T21 may exhibit a broad range of phenotypes, including congenital heart diseases, hypotonia, and neurodevelopmental disorders; notably, T21 is the most common genetic cause of intellectual disability[15–17]. Common neurodevelopmental symptoms associated with T21 include differences in working memory and attention span, and delayed language and motor skill development, which are primarily controlled by the frontal and temporal lobes of the neocortex, respectively[17]. In the neonatal T21 brain, these regions have a thinner neocortex, with reduced neuron and oligodendrocyte abundance, while astrocyte abundance is increased as compared to healthy infants[17]. It is hypothesized that this difference results from an earlier transition of radial glia from neurogenesis to gliogenesis, with oligodendrocyte precursor cells giving rise to more astrocytes than oligodendrocytes in the developing T21 brain as compared to euploid[18–20]. However, there is minimal research surrounding the molecular mechanisms and dynamics underpinning the observed differences in the fetal T21 neocortex.

1.1. Study rationale

The molecular mechanisms underpinning intellectual disability and neocortical development in T21 are not well understood. The GDF15 signalling pathway may play a role in fetal development of the neocortex in individuals with T21, though this requires investigation. Identifying differing developmental pathways in T21 is essential to expand

our understanding of this disorder and develop support programs for intellectual disability in individuals with T21.

1.2. Objectives

1. Investigate patterns of progenitor cell abundance and cytoarchitectural organization in euploid and T21 fetal human neocortices; and,
2. Examine the expression profile of genes in the GDF15 signalling pathway during early to mid-gestation in euploid and T21 neocortices.

1.3. Hypotheses and predictions

With respect to objective 1, I hypothesized that T21 alters the cytoarchitectural organization of the fetal human neocortex and predicted that NPC abundance is lower in the fetal T21 neocortex relative to age-matched euploid neocortices. This prediction is corroborated by previous literature implicating T21 in reducing bRG abundance and neocortical thickness, and delaying neurogenesis in human and mouse (*Mus musculus*) models of the disorder[21,22].

With respect to objective 2, I hypothesized that the GDF15 signalling pathway is differently regulated in the T21 fetal human neocortex, and predicted that the mRNA transcript levels of *DACH1*, *SHROOM3*, and *SEMA5A* will be reduced, while *GPC6* transcript levels will be elevated in the T21 fetal neocortex compared to euploid. This prediction is supported by observations from a GDF15 knock-out mouse model, in which NPC abundance was reduced relative to controls, and target genes including *Dach1*, *Gpc6*, *Shroom3*, and *Sema5a* were shown to be regulated by GDF15, highlighting the possible influence of the GDF15 pathway on neurogenesis[23].

2. Materials and Methods

2.1. Study design

2.1.1. Experimental approach 1: Immunofluorescence of neural progenitor cell abundance in euploid and T21 neocortices

To address objective 1 and examine the cytoarchitectural differences in the T21 fetal brain as compared to euploid controls, if any, immunofluorescence and imaging of these neocortices was carried out. Fixed euploid and T21 neocortical tissues from various gestational ages were stained and visualized for the proteins of interest:

- To test for cytoarchitectural differences in NPC organization in the developing neocortex, the expression of SRY-box transcription factor 2 (SOX2), an apical and basal radial glial cell marker, and homeodomain-only protein X (HOPX), a basal radial glial cell marker, were studied[24,25]. The expression of phosphorylated vimentin (PVIM), a mitotic cell marker, and SATB homeobox 2 (SATB2), a marker of layer II-V callosally projecting neurons in the mature neocortex, was visualized to observe differences in NPC proliferation and differentiation, respectively[26,27].
- As radial glia may differentiate to form macroglia, the expression of oligodendrocyte transcription factor 1 (OLIG1), an oligodendrocyte precursor cell marker, and S100 calcium binding protein B (S100B), an astrocyte marker, were visualized to observe differences in gliogenesis in the T21 neocortex as compared to the euploid neocortex[3,28,29]. Moreover, *S100B* and *OLIG1* genes are localized on chromosome 21 in humans, making these genes of interest and relevance in the study of T21 due to their increased gene dosage[29,30].

- As the GDF15 signalling pathway is of interest in the context of T21, the expression of potential downstream targets GPC6 and DACH1 was visualized.

Images of cortical columns from these neocortices were collected using a Zeiss Laser Confocal LSM 700 microscope, and cell counts of these targets in the oSVZ were quantified.

2.1.2. Experimental approach 2: Gene expression in euploid and T21 neocortices

To address objective 2 and examine gene expression profiles throughout gestation in fetal euploid and T21 neocortices, real-time quantitative polymerase chain reaction (RT-qPCR) assays were conducted. RNA was extracted from frozen T21 and euploid control neocortices, followed by complementary DNA (cDNA) synthesis. cDNA was prepared for RT-qPCR assays using a reagent kit (see below), and primers were selected to quantify the expression levels of relevant genes of interest:

- As radial glia may differentiate to form macroglia, the expression of oligodendrocyte precursor cell markers *OLIG1* and oligodendrocyte transcription factor 2 (*OLIG2*; also localized on chromosome 21), and astrocyte marker *S100B* was quantified to test for differences in gliogenesis in the T21 neocortex as compared to the euploid neocortex[3,28,29].
- As the GDF15 signalling pathway is of interest in the context of T21, gene expression of the potential downstream targets *GPC6*, *DACH1*, *SHROOM3*, and *SEMA5A* was quantified by RT-qPCR. Further, expression levels of the gene encoding the GDF15 receptor, *GFRAL*, were also quantified to compare receptor expression in the fetal euploid and T21 neocortex.

- To normalize gene expression levels to a reference value, glyceraldehyde-3-phosphate dehydrogenase (*GAPDH*) and beta-actin (*ACTB*) were used as housekeeping genes.

Quantification cycle values (i.e., the PCR cycle number at which a predefined fluorescence threshold is crossed) were used to quantify gene expression levels relative to the geometric mean of *GAPDH* and *ACTB* expression.

2.2. Fetal human neocortical tissue

To investigate the potential influence of T21 on early neural development, this project used neocortical tissue from fetuses diagnosed with the disorder to those without. Fixed (euploid: $n = 2$; T21: $n = 3$) and frozen (euploid: $n = 5$; T21: $n = 3$) fetal human neocortical tissue samples from T21 fetuses and age-matched euploid fetuses were obtained from the Human Developmental Biology Resource at various developmental ages ranging from PCW 10 to PCW 20 (Table 1). Upon receipt of neocortical tissue, fixed tissues were saturated in 30% sucrose at 4°C overnight, then embedded in Optimal Cutting Temperature compound and flash frozen in liquid nitrogen[31]. Embedded tissues were stored at -20°C; frozen tissues were stored at -80°C.

Research studies and experimental procedures in this project have been reviewed by the University of Manitoba (UM) Health Research Board (HREB) and were found to be acceptable on ethical grounds for research (Ethics HS26312 (H2024:041)).

Table 1. Preservation method, developmental age, genotype, and sample sizes of fetal neocortical tissue samples used for data collection.

Preservation	Developmental age (PCW)	Genotype	Sample size (*n*)
Fixed	12	Euploid	1
	13	T21	1
	16	Euploid	1
	17	T21	1
	20	T21	1
Frozen	12	Euploid	3
	12	T21	1
	13	Euploid	1
	14	T21	1
	15	Euploid	1
	17	T21	1

2.3. Immunofluorescence and imaging

Embedded neocortices (Table 1) were cryosectioned using a cryotome (Thermo Scientific #A78910100) into 20 µm to 50 µm sections. Slices were mounted onto Superfrost™ Plus Microscope Slides (Fisher Scientific # 22-037-246) and stored at -20°C for storage until immunofluorescence staining. Immunofluorescence staining was performed as described previously[31]. Slides were thawed for 10 to 20 minutes prior to staining and washed in phosphate-buffered saline (pH = 7.4) twice for 5 minutes per wash. Antigen retrieval was performed by incubating slides in 0.01 M citrate buffer (pH = 6.0) at 70°C for 1 hour. Slides were permeabilized in 0.3% TritonX100 in PBS at room temperature for 30 minutes. Paraformaldehyde quenching in 0.1 M glycine buffer (pH =

7.4) was performed for 30 minutes, followed by incubation in a blocking buffer solution (2% gelatin, 0.3% TritonX100, 300 mM NaCl in PBS) three times at room temperature for 30 to 60 minutes. Slides were incubated overnight in humid conditions at 4°C with primary antibodies (Table 2) in blocking buffer. Slides were washed in blocking solution three times for 20 minutes per wash, followed by incubation for 1 hour in humid conditions at room temperature with secondary antibodies (Table 2) and 4',6-diamidino-2-phenylindole (DAPI), diluted 500-fold and 1000-fold, respectively, in blocking buffer. Slides were washed in PBS at room temperature three times for 20 minutes per wash, prior to being mounted with Mowiol using Fisherbrand™ Rectangular Cover Glasses (Fisher Scientific #12541032CA).

Images of whole hemispheres from IF-stained neocortex were captured using the EVOS M7000 Imaging System (Fisher Scientific #AMF7000HCA) with a 10X objective. Images of representative cortical columns from each IF-stained neocortex were captured using the Zeiss Laser Confocal LSM700 microscope with a Zeiss Plan-Apochromat 20X objective, maintaining consistent microscope settings (i.e., laser power, gain, and pinhole aperture) between images taken for the same target. Images were stitched together using Fiji (Is Just ImageJ) to generate images of a full cortical column[32].

Table 2. Primary and secondary antibodies used for immunofluorescence. SOX2: SRY-box transcription factor 2; HOPX: homeodomain-only protein X; PVIM: phosphorylated vimentin; GPC6: glypican 6; DACH1: dachshund family transcription factor 1; SATB2: SATB homeobox 2; OLIG1: oligodendrocyte transcription factor 1; S100B: S100 calcium binding protein B; AF: Alexa Fluor.

	Target	Dilution	Vendor	Catalog number
Primary antibodies	SOX2	1:500	R&D Systems	AF2018
	HOPX	1:500	Invitrogen	PA5-90538
	PVIM	1:500	MBL Life Science	D076-3
	GPC6	1:250	Invitrogen	703424
	DACH1	1:500	Abcam	AB226176
	SATB2	1:100	Abcam	AB51502
	OLIG1	1:400	Invitrogen	MA523954
	S100B	1:500	Abcam	AB868
Secondary antibodies	Rabbit AF488	1:500	Invitrogen	A32790
	Goat AF555	1:500	Invitrogen	A-21432
	Mouse AF555	1:500	Invitrogen	A31570

2.4. Quantification

Cell counting of SOX2, PVIM, DACH1, OLIG1, S100B, and DAPI-positive cells was performed in Fiji. Standardized microscopic fields were used to quantify these markers in the oSVZ of cortical columns of PCW 12 and PCW 13 samples (50 µm by 50 µm) and PCW 16, PCW 17, and PCW 20 samples (100 µm by 100 µm). Quantifications of technical triplicates of each oSVZ field were performed blindly.

2.5. RNA extraction and cDNA synthesis

RNA extractions from eight frozen fetal neocortices (Table 1) were carried out using the PureLink™ RNA Mini Kit (Invitrogen #12183018A), following the manufacturer's instructions for purification from animal tissues (Pub. No. MAN0019346); frozen tissues were homogenized using a rotor-stator homogenizer, subject to DNase treatment, and RNA was eluted in 50 µL of UltraPure™ DNase/RNase-Free Distilled Water (Invitrogen #10977-015). RNA yields and quality were quantified using the NanoDrop Lite Plus Spectrophotometer (Thermo Scientific #NDLPLUSGL) by measuring sample absorbance at 260 nm. RNA was stored at -80°C until use for cDNA synthesis.

cDNA was synthesized from 0.15 µg of extracted RNA using the Maxima First Strand cDNA Synthesis Kit for RT-qPCR (Thermo Scientific #K1642) following the manufacturer's instructions (Pub. No. MAN0012718). cDNA was diluted 20-fold in UltraPure™ DNase/RNase-Free Distilled Water (Invitrogen #10977-015) for RT-qPCR use.

2.6. Real-time quantitative polymerase chain reaction

RT-qPCR assays were prepared using PowerTrack™ SYBR Green Master Mix (Applied Biosystems #A46109) following the manufacturer's instructions for a 10 µL final reaction volume with minor modifications; assays were prepared without the optional Yellow Sample Buffer, and 3 µL of cDNA was used. Primers used for this study (Table 3) were previously designed by other members of the Xing Lab[23]. Primers were diluted to a final working concentration of 400 nM, and nuclease-free water was used to achieve a final reaction volume of 10 µL, as per the manufacturer's instructions.

Table 3. Primers used for RT-qPCR. *GAPDH*: glyceraldehyde-3-phosphate dehydrogenase; *ACTB*: beta-actin; *GFRAL*: glial-cell derived neurotrophic factor family receptor alpha-like; *GPC6*: glypican 6; *DACH1*: dachshund family transcription factor 1; *SHROOM3*: shroom family 3; *SEMA5A*: semaphorin 5A; *OLIG1*: oligodendrocyte transcription factor 1; *OLIG2*: oligodendrocyte transcription factor 2; *S100B*: S100 calcium binding protein B; F: forward primer; R: reverse primer.

Gene	**Primer sequence (5' to 3')**
GAPDH	F: AAGGTGAAGGTCGGAGTCAA R: AATGAAGGGGTCATTGATGG
ACTB	F: CGTCTTCCCCTCCATCGTG R: TACTTCAGGGTGAGGATGCC
GFRAL	F: AAAGGGATGTGGTCCTGTTTGG R: GTATGGCTGCTTGGCACTGTTT
GPC6	F: TCTTGGTGGCAGAGCGACT R: TGGAGCAGGTTTGGGCTGAC
DACH1	F: GGCAATGAGCCAGATGAACCA R: CTGCTGCGATGTGATGATGGG
SHROOM3	F: GCTTTTGGGGCAAGACAGTGG R: AACGAGGGGTGAGATGGTGGA
SEMA5A	F: AGGCTGCAATGTGGAGTACC R: CGGGCTTTGCATGTGTATCG
OLIG1	F: GCGTATCCAGTGTTTTGTCGCA R: GCAAGGCGGTTGGTTTTCGT

OLIG2	F: AGAAGCAAATGACAGAGCCG R: CATCCATGGCGATGTTGAGG
S100B	F: GAAGGGAGGGAGACAAGCACA R: GTGGCAGGCAGTAGTAACCAT

A technical triplicate was run for each cDNA sample alongside a negative control per gene. Expression levels of these genes were quantified relative to the housekeeping genes – *GAPDH* and *ACTB* – using the QuantStudio™ 3 Real-Time PCR System (Applied Biosystems #A28567).

2.7. Statistical analysis

Excel (Microsoft version 2604) and Prism (Graphpad version 10.6.1) were used for data calculation and statistical analysis of cell quantifications from immunofluorescence data and relative gene expression from RT-qPCR data. Normality of the data was assessed using the Kolmogorov–Smirnov and the Shapiro–Wilk tests. A two-tailed, unpaired t-test with a significance level (α) of 0.05 was used to compare differences in the mean gene expression levels of normally distributed euploid controls and T21 samples. If the mean gene expression levels of the samples were not normally distributed, a nonparametric Mann-Whitney U test was performed to compare differences in gene expression levels. Error bars indicate the standard error of the mean (SEM).

3. Results

3.1. Elevated mRNA expression of chromosome 21 genes in trisomy 21 neocortices

RT-qPCR was used to examine the expression profile of *OLIG1*, *OLIG2*, and *S100B* to confirm the genotype of each neocortex used for RT-qPCR analyses, and to investigate potential aberrations in gliogenesis. These genes are localized on chromosome

21, and, as such, their elevated expression supports a diagnosis of T21. Further, these genes are involved in oligodendrocyte (*OLIG1*, *OLIG2*) and astrocyte (*S100B*) proliferation and differentiation; their expression may thus be indicative of altered gliogenesis. *OLIG1* (P = 0.0143), *OLIG2* (P = 0.0021), and *S100B* (P = 0.0021) showed significant higher expression in T21 neocortices compared to euploid (Fig. 2A-C). These high expression levels further validate the T21 genotype of these neocortices and may potentially contribute aberrations in gliogenesis. Karyotyping of each neocortex was performed by the Human Developmental Biology Resource and confirmed the genotype of each neocortex.

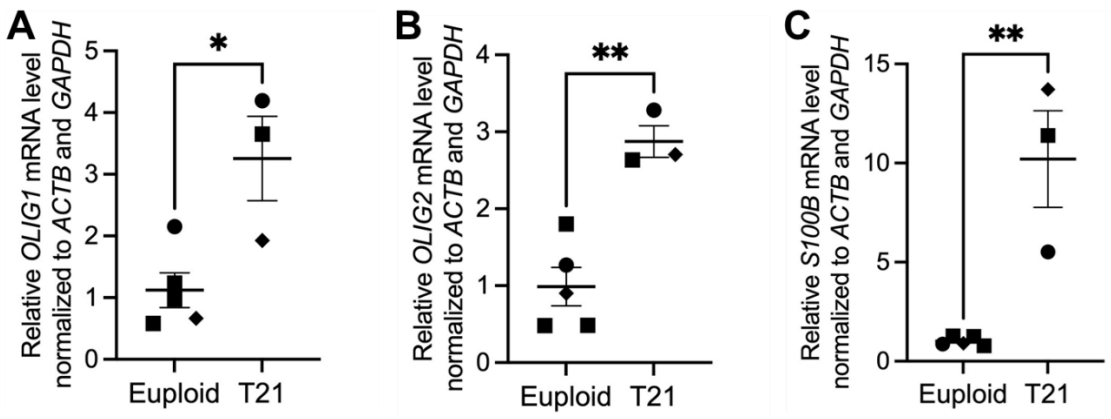

Figure 2. Relative mRNA expression levels of glial target genes in euploid (n=5) and T21 (n=3) fetal human neocortices. RT-qPCR data of *OLIG1* (A), *OLIG2* (B), and *S100B* (C) were normalized to *ACTB* and *GAPDH* expression levels. Different symbols in each group indicate individual biological samples. Squares: PCW 12; diamonds: PCW 13 (euploid) and PCW 14 (T21); circles: PCW 15 (euploid) and PCW 17 (T21). * $p < 0.05$; ** $p < 0.01$. Error bars, SEM.

3.2. Neocortex cytoarchitecture and neural and glial progenitor cell abundance may be altered at post-conceptional week 13

To test for potential effects of T21 on NPC abundance in the fetal neocortex, immunofluorescent staining and confocal microscopy imaging of NPC markers were performed; namely, SOX2, an apical radial glia and bRG marker, and HOPX, a bRG marker. To visualize the different cortical zones within the developing neocortex, a whole cerebral hemisphere was stained for these markers alongside DAPI, a nuclear marker that binds to double-stranded DNA, effectively staining all cells in the neocortex (Fig. 3A)[33]. A full cortical column within this hemisphere was imaged, and DAPI distribution was used to identify the different cortical zones (Fig. 3B): the VZ is a compact layer of various NPCs, primarily apical radial glia; the iSVZ and oSVZ are less tightly packed than the VZ, and primarily house bRG and basal intermediate progenitors. These regions exhibit high expression of SOX2, as it is both an apical and basal radial glia marker; HOPX did not appear to successfully stain bRG in the iSVZ and oSVZ to distinctively delineate it from the VZ within a cortical column (Fig. 3B). The intermediate zone is loosely packed, whereas the cortical plate is densely packed, similar to the VZ, but lacks SOX2 expression (Fig. 3B). When comparing the PCW 12 euploid oSVZ to the PCW 13 T21 oSVZ, fewer SOX2-positive cells appeared to be present in the T21 oSVZ (Fig. 4A-B). By PCW 16 and PCW 17 in the euploid and T21 oSVZ, respectively, the abundance of SOX2-positive cells appeared to decrease further, with the lowest abundance at PCW 20 of the T21 oSVZ (Fig. 4C-E). Importantly, when comparing the abundance of SOX2-positive cells in the euploid and T21 oSVZ across these time points, there was no significant difference between the groups (Fig. 4F-I), potentially due to developmental dynamics at different

stages. It should be clarified that HOPX did not appear to successfully stain bRG in the euploid and T21 oSVZ (Fig. 4A-E).

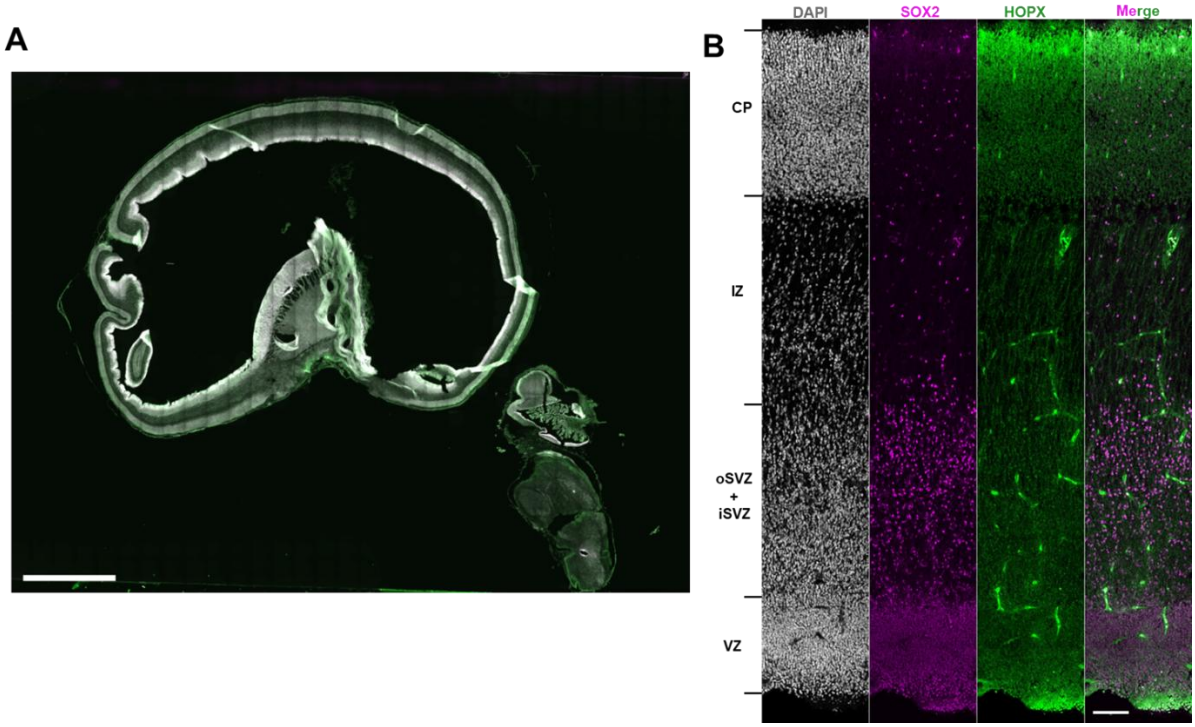

Figure 3. Homeodomain-only protein X (HOPX; green) and SRY-box transcription factor 2 (SOX2; magenta) expression throughout the fetal euploid PCW 12 neocortex. DAPI (grey): 4'-6-diamidino-2-phenylindole; VZ: ventricular zone; iSVZ: inner subventricular zone; oSVZ: outer subventricular zone; IZ: intermediate zone; CP: cortical plate. (A) Expression throughout a coronal section of the brain at PCW 12. Scale bar, 500 μm. (B) Expression throughout a cortical column within the whole hemisphere of the brain. Scale bar, 100 μm.

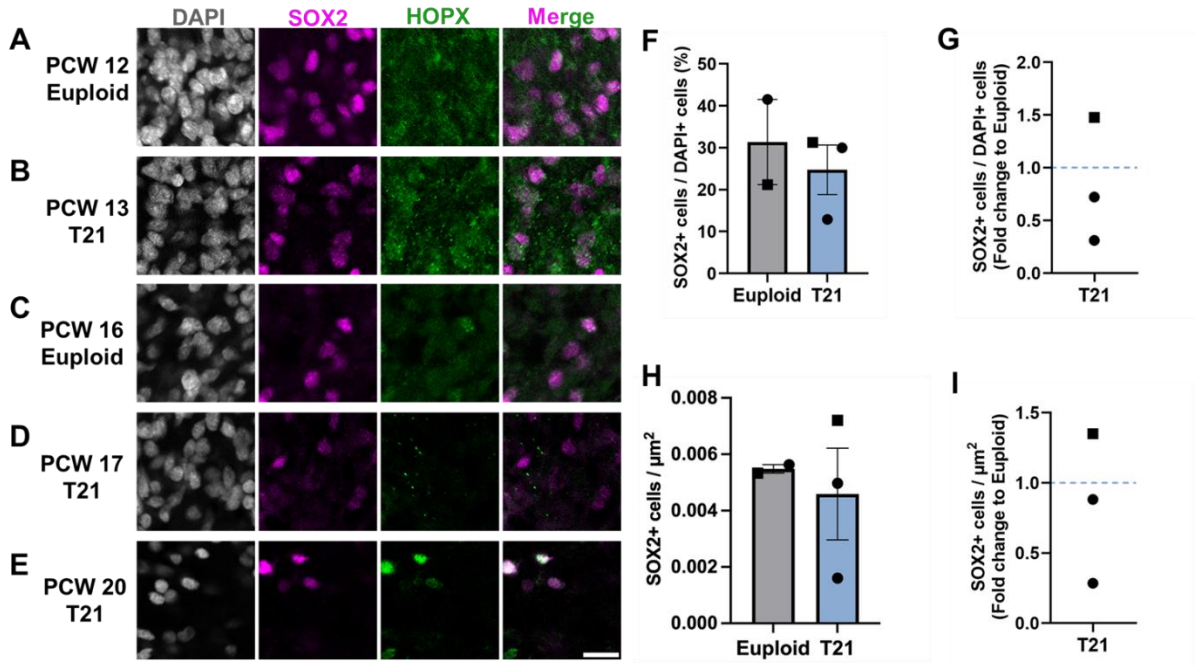

Figure 4. Homeodomain-only protein X (HOPX; green) and SRY-box transcription factor 2 (SOX2; magenta) expression in the fetal euploid and T21 oSVZ. DAPI (grey): 4'-6-diamidino-2-phenylindole. Scale bar, 15 µm. (A) Expression in the euploid oSVZ at PCW 12. (B) Expression in the T21 oSVZ at PCW 13. (C) Expression in the euploid oSVZ at PCW 16. (D) Expression in the T21 oSVZ at PCW 17. (E) Expression in the T21 oSVZ at PCW 20. Quantification of SOX2-positive cells within the oSVZ (F) and fold-change relative to euploid (G) normalized to the total number of cells; quantification of SOX2-positive cells within the oSVZ (H) and fold-change relative to euploid (I) normalized to area (μm^2). Different symbols in each group indicate individual biological samples. Squares: PCW 12 (euploid) and PCW 13 (T21); circles: PCW 16 (euploid), PCW 17 (T21), and PCW 20 (T21). Error bars, SEM.

A mitotic cell marker, PVIM, was stained to determine the effects of T21 on NPC proliferation. The expression of PVIM appeared to be slightly increased in the VZ, iSVZ,

and oSVZ of the PCW 13 T21 neocortex as compared to euploid (Fig. 5A-B, A'-B'). At PCW 16-20, PVIM expression appeared to be comparably negligible throughout the VZ, iSVZ, and oSVZ in both euploid and T21 neocortices (Fig. 5C-E, C'-E'). However, there was no significant difference in the abundance of PVIM-positive cells between the euploid and T21 oSVZ across these timepoints (Fig. 5F-I).

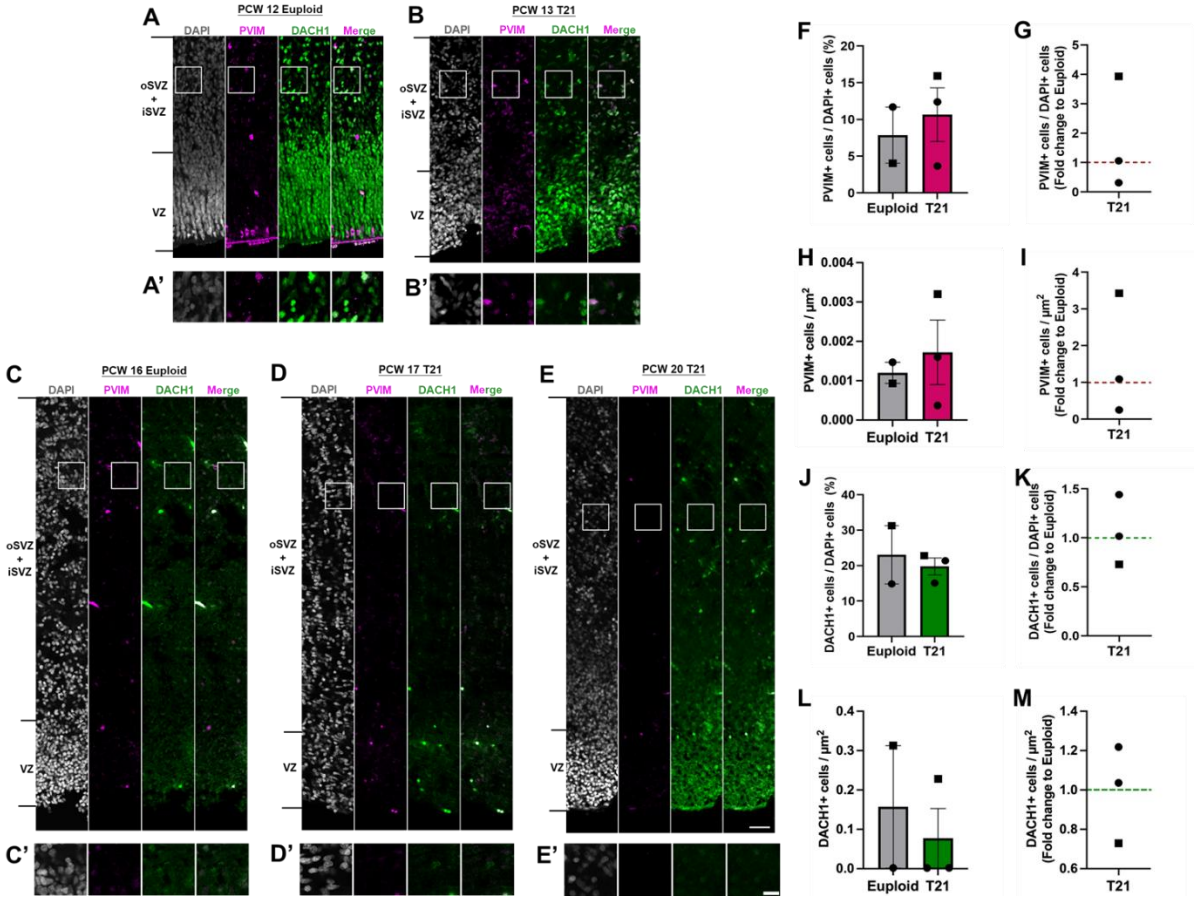

Figure 5. Dachshund family transcription factor 1 (DACH1; green) and phosphorylated vimentin (PVIM; magenta) expression in the fetal euploid and T21 neocortex and oSVZ. DAPI (grey): 4'-6-diamidino-2-phenylindole; VZ: ventricular zone; iSVZ: inner subventricular zone; oSVZ: outer subventricular zone. Scale bar in full neocortical columns, 40 µm. Scale bar in oSVZ view, 15 µm. Expression in the euploid neocortex (A)

and oSVZ (A') at PCW 12; expression in the T21 neocortex (B) and oSVZ (B') at PCW 13; expression in the euploid neocortex (C) and oSVZ (C') at PCW 16; expression in the T21 neocortex (D) and oSVZ (D') at PCW 17; expression in the T21 neocortex (E) and oSVZ (E') at PCW 20. Quantification of PVIM-positive cells within the oSVZ (F) and fold-change relative to euploid (G) normalized to the total number of cells; quantification of PVIM-positive cells within the oSVZ (H) and fold-change relative to euploid (I) normalized to area (μm^2). Quantification of DACH1-positive cells within the oSVZ (J) and fold-change relative to euploid (K) normalized to the total number of cells; quantification of DACH1-positive cells within the oSVZ (L) and fold-change relative to euploid (M) normalized to area (μm^2). Different symbols in each group indicate individual biological samples. Squares: PCW 12 (euploid) and PCW 13 (T21); circles: PCW 16 (euploid), PCW 17 (T21), and PCW 20 (T21). Error bars, SEM.

A callosally projecting neuron marker, SATB2, was stained to determine the effects of T21 on NPC differentiation into neurons. SATB2 expression appeared to be minimal in the PCW 12 euploid neocortex, with seemingly increased expression in the PCW 13 T21 VZ, iSVZ, and oSVZ (Fig. 6A-B, A'-B'). SATB2 expression appeared to increase in these regions of the euploid neocortex by PCW 16, with seemingly comparable expression levels in the PCW 17 T21 neocortex; these regions appeared to exhibit slightly greater SATB2 expression in the PCW 20 T21 neocortex (Fig. 6C-E, C'-E'). When quantifying SATB2-positive cells in these regions, there was no significant difference in the abundance of these cells between the euploid and T21 oSVZ (Fig. 6F-I). Collectively, these results suggest that T21 may impact NPC proliferation and differentiation most at PCW 13.

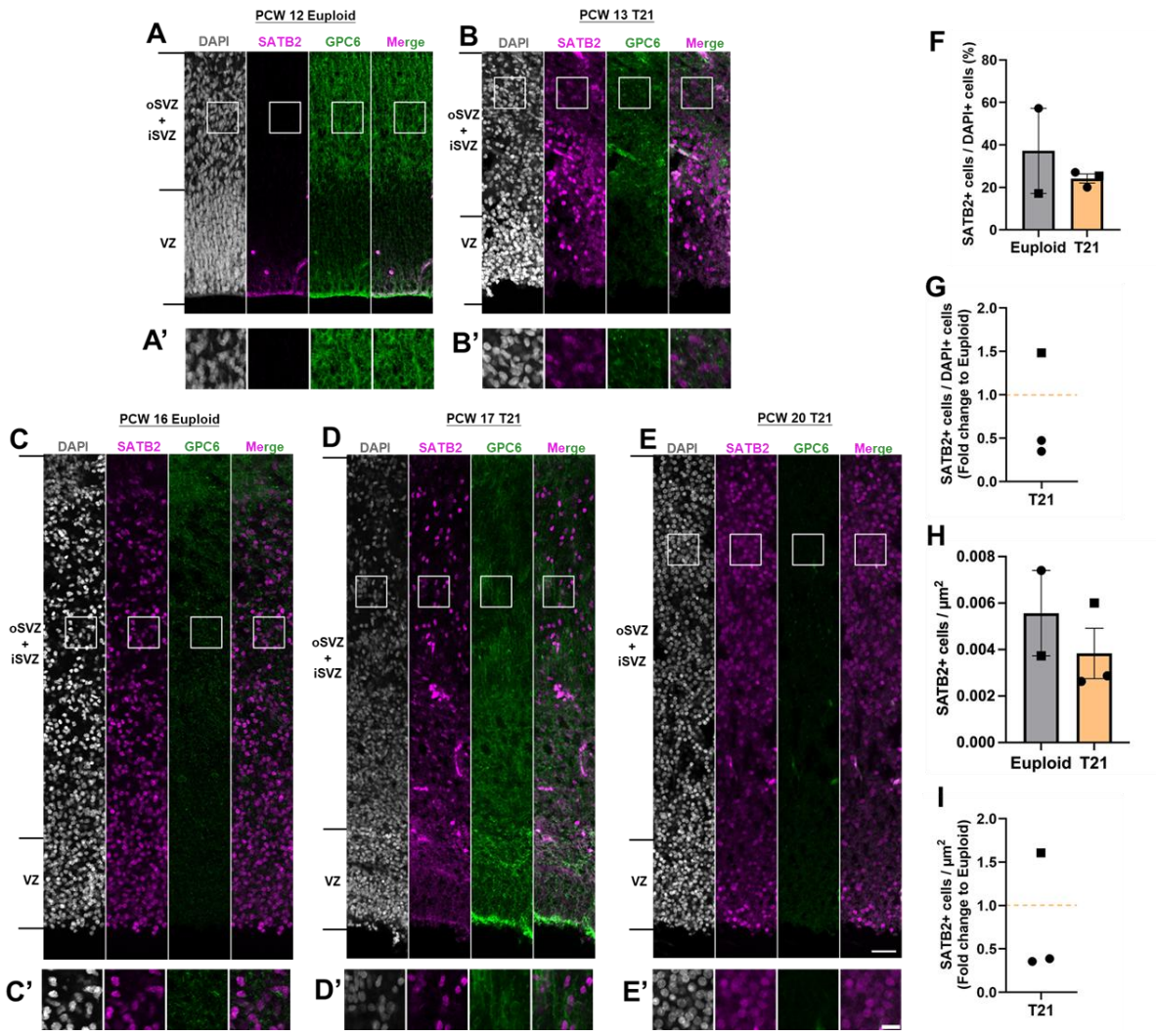

Figure 6. Glypican 6 (GPC6; green) and SATB homeobox 2 (SATB2; magenta) expression in the fetal euploid and T21 neocortex and oSVZ. DAPI (grey): 4'-6-diamidino-2-phenylindole; VZ: ventricular zone; iSVZ/oSVZ: inner/outer subventricular zone. Scale bar in full neocortical columns, 40 µm. Scale bar in oSVZ view, 15 µm. Expression in the euploid neocortex (A) and oSVZ (A') at PCW 12; expression in the T21 neocortex (B) and oSVZ (B') at PCW 13; expression in the euploid neocortex (C) and oSVZ (C') at PCW 16; expression in the T21 neocortex (D) and oSVZ (D') at PCW 17; expression in the T21 neocortex (E) and oSVZ (E') at PCW 20. Quantification of SATB2-

positive cells within the oSVZ (F) and fold-change relative to euploid (G) normalized to the total number of cells; quantification of SATB2-positive cells within the oSVZ (H) and fold-change relative to euploid (I) normalized to area (μm^2). Different symbols in each group indicate individual biological samples. Squares: PCW 12 (euploid) and PCW 13 (T21); circles: PCW 16 (euploid), PCW 17 (T21), and PCW 20 (T21). Error bars, SEM.

To investigate the effects of T21 on gliogenesis, glial markers were stained. An oligodendrocyte precursor cell marker, OLIG1, was stained to determine the effects of T21 on NPC differentiation into oligodendrocytes. OLIG1 expression appeared to to be low in the PCW 12 euploid neocortex, with seemingly increased expression in the PCW 13 T21 VZ, iSVZ, and oSVZ (Fig. 7A-B, A'-B'). OLIG1 expression appears to increase in these regions of the euploid neocortex by PCW 16, with seemingly comparable expression levels in the PCW 17 and PCW 20 T21 neocortices (Fig. 7C-E, C'-E'). When quantifying OLIG1-positive cells in these regions, there was no significant difference in the abundance of these cells between the euploid and T21 oSVZ (Fig. 7F-I).

Moreover, an astrocyte marker, S100B, was stained to determine the effects of T21 on NPC differentiation into astrocytes. While S100B-positive cell abundance appeared to be low in the euploid neocortex at all gestational ages, the abundance of these cells appeared to be lower in T21, regardless of gestational age (Fig. 7A-E, A'-E'). When quantifying S100B-positive cells in these regions, there was a significant decrease in the abundance of these cells between the euploid and T21 oSVZ when standardized for both total number of cells ($P = 0.0019$) and area ($P = 0.0202$), with a 0.19-fold ($P = 0.0049$) and 0.21-fold difference ($P = 0.0038$), respectively (Fig. 7J-M). These results indicate that T21 affects NPC differentiation into astrocytes more than into oligodendrocytes.

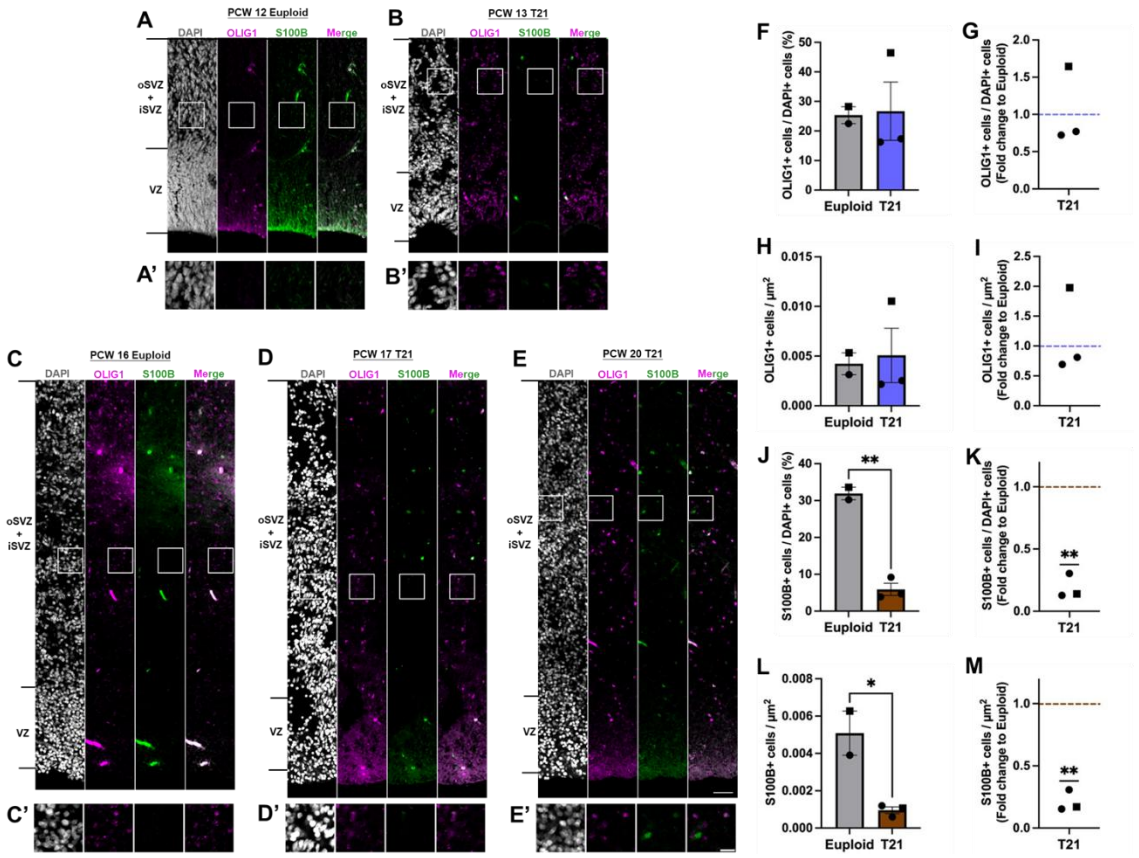

Figure 7. Oligodendrocyte transcription factor 1 (OLIG1; magenta) and S100 calcium binding protein B (S100B; green) expression in the fetal euploid and T21 neocortex and oSVZ. DAPI (grey): 4'-6-diamidino-2-phenylindole; VZ: ventricular zone; iSVZ: inner subventricular zone; oSVZ: outer subventricular zone. Scale bar in full neocortical columns, 40 µm. Scale bar in oSVZ view, 15 µm. Expression in the euploid neocortex (A) and oSVZ (A') at PCW 12; expression in the T21 neocortex (B) and oSVZ (B') at PCW 13; expression in the euploid neocortex (C) and oSVZ (C') at PCW 16; expression in the T21 neocortex (D) and oSVZ (D') at PCW 17; expression in the T21 neocortex (E) and oSVZ (E') at PCW 20. Quantification of OLIG1-positive cells within the oSVZ (F) and fold-change relative to euploid (G) normalized to the total number of cells; quantification of OLIG1-positive cells within the oSVZ (H) and fold-change relative to euploid (I)

normalized to area (μm^2). Quantification of S100B-positive cells within the oSVZ (J) and fold-change relative to euploid (K) normalized to the total number of cells; quantification of S100B-positive cells within the oSVZ (L) and fold-change relative to euploid (M) normalized to area (μm^2). Different symbols in each group indicate individual biological samples. Squares: PCW 12 (euploid) and PCW 13 (T21); circles: PCW 16 (euploid), PCW 17 (T21), and PCW 20 (T21). * $p < 0.05$; ** $p < 0.01$. Error bars, SEM.

3.3. Expression of growth differentiation factor 15 targets may be altered at post-conceptional week 13

Immunofluorescent staining and confocal microscopy imaging of various GDF15 targets were carried out in fetal euploid and T21 neocortices to compare differences in their expression and localization. DACH1 appeared to be localized to the VZ, iSVZ, and oSVZ at PCW 12 to PCW 13, with a seemingly decreased DACH1-positive cell abundance in T21 oSVZ as compared to euploid (Fig. 5A-B, A'-B'). DACH1 expression appeared to decrease at PCW 16-20, with seemingly no expression throughout the euploid and T21 VZ, iSVZ, and oSVZ (Fig. 5C-E, C'-E'). Interestingly, comparing the abundance of DACH1-positive cells between the euploid and T21 oSVZ across these timepoints revealed no significant difference between these groups (Fig. 5J-M).

GPC6 appeared to be primarily localized to the oSVZ at PCW 12 euploid and PCW 13 T21 neocortices, with visibly lower GPC6 expression in the PCW 13 T21 oSVZ (Fig. 6A-B, A'-B'). By PCW 16 in the euploid neocortex, GPC6 expression within the VZ, iSVZ, and oSVZ appeared to notably diminish (Fig. 6C, C'). However, these regions appeared to continue expressing GPC6 at PCW 17 in the T21 neocortex, with GPC expression appearing to later decrease to euploid PCW 16 levels by PCW 20 in T21 (Fig.

6D-E, D'-E'). Therein, these results highlight the potential influence of T21 on these GDF15 targets, GPC6 and DACH1, and further imply this pathway's roles on fetal neurodevelopment.

3.4. Elevated expression of *SEMA5A*, a growth differentiation factor 15 target

RT-qPCR was used to examine the expression profile of genes involved in the GDF15 signalling pathway at various gestational ages in euploid and T21 neocortices. There was no significant difference in the expression of most genes involved in the GDF15 signalling pathway (*GFRAL*, *GPC6*, *DACH1*, *SHROOM3*) between euploid and T21 neocortices; however, *SEMA5A* showed a significantly higher expression in the T21 neocortex as compared to euploid tissues (P = 0.0357) (Fig. 8A-E).

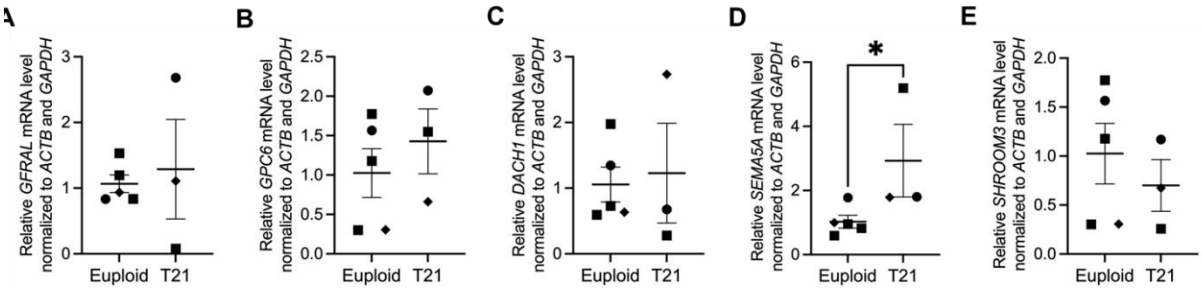

Figure 8. Relative mRNA expression levels of GDF15 target genes in euploid (n=5) and T21 (n=3) fetal human neocortices. RT-qPCR data of *GFRAL* (A), *GPC6* (B), *DACH1* (C), *SEMA5A* (D), and *SHROOM3* (E) were normalized to *ACTB* and *GAPDH* expression levels. Different symbols in each group indicate individual biological samples. Squares: PCW 12; diamonds: PCW 13 (euploid) and PCW 14 (T21); circles: PCW 15 (euploid) and PCW 17 (T21). * $p < 0.05$. Error bars, SEM.

4. Discussion

The goal of this study was to examine the cytoarchitecture of the neocortex and regulation of the GDF15 pathway in the fetal T21 neocortex at various gestational ages in comparison to the euploid neocortex. Here, findings from this study demonstrate that the GDF15 pathway plays a potential role in early fetal neurodevelopment, particularly in the context of T21. Specifically, a downstream gene target of GDF15, *SEMA5A*, is differentially expressed in T21, while other GDF15 protein targets, DACH1 and GPC6, may be differentially expressed in early T21 neurodevelopment at PCW 12. These results suggest that an altered GDF15 signalling pathway may affect neurodevelopment in T21. Four major findings warrant further discussion.

4.1. Elevated expression of glial genes on chromosome 21 may contribute to altered neural development

The elevated expression of genes regulating gliogenesis, *OLIG1*, *OLIG2*, and *S100B*, suggests altered glial proliferation or differentiation in T21. Elevated *OLIG1* and *OLIG2* expression in the T21 neocortex is corroborated by previous studies[30]. The correspondence of this higher expression level to altered abundance or cytoarchitectural organization of oligodendrocyte progenitor cells in the embryonic T21 neocortex was not consistent; the abundance of cells positive for OLIG1 did not appear to differ between euploid and T21 oSVZs, while the abundance of cells positive for S100B was significantly reduced in T21 across all gestational ages. While few studies have investigated the effects of T21 on OLIG1-positive cell abundance, the results presented here are inconsistent with another study that reported an increase in the abundance of cells expressing S100B[34]. This discrepancy may be attributed to the limited sample size of one

biological replicate per gestational age used for immunofluorescence in this study, due to limitations in obtaining human tissue. While OLIG2-positive cells were not studied by immunofluorescence, increased OLIG2 expression has been shown to decrease NPC proliferation and neuronal abundance[35]. A decrease in NPC proliferation, alongside the effects of elevated *S100B*, may explain the reduction in the thickness of the neocortex observed in newborns with T21, making future studies into these cells of notable importance[17].

S100B expression was significantly higher (~10-fold) in the embryonic T21 neocortex, a finding that is also corroborated by existing literature[36]. S100B promotes the growth of neuronal projections such as axons, dendrites, and dendritic spines, collectively known as neurites, and regulates synaptic plasticity, with previous research showing that an elevation in its expression level drives the early transition of bRG to a gliogenic fate[29,34]. By contrast, a potential decrease in the abundance of SOX2-positive cells, which include bRG, was found at PCW 17 and PCW 20 in T21 relative to euploid; this potential reduction does not seem to be correlated with the earlier transition of these cells to a gliogenic fate driven by S100B, as seen by the comparable and reduced abundance of cells positive for OLIG1 and S100B, respectively. Elevated *S100B* expression has also been shown to increase neurite dystrophy and reactive oxygen species production, resulting in increased apoptosis of NPCs[29,37,38]. Thus, the potential reduction in SOX2-positive radial glia in T21 at PCW 17 and PCW 20 may also be attributed to increased cellular apoptosis rather than a transition to gliogenesis. Quantification of the expression of pro-apoptosis genes or proteins such as the Bcl-2 or caspase families in the T21 neocortex may provide insight into the mechanisms by which radial glia are affected by

this syndrome[39,40]. Likewise, given that infants with T21 exhibit reductions in the abundance and size of dendritic spines, the effects of S100B on neurite dystrophy should be examined, as dendritic spines are a proxy for synaptic contacts, and any developmental differences in synapse formation may play a role in intellectual disability arising from altered synaptogenesis observed in T21[17].

4.2. Early differentiation may contribute to potential reductions in NPC abundance

The oSVZ of euploid and T21 neocortices, ranging from PCW 12 to PCW 20, were examined for the abundance of cells expressing SOX2, a radial glia marker, notably bRG, a class of radial glia that exhibits highly proliferative capacities in humans. Unlike other NPCs, bRG may commit to either neurogenic or gliogenic fates, making these cells particularly interesting in fetal development of the human neocortex[1,2,6,7]. The abundance of SOX2-positive radial glia was not significantly different between euploid and T21 samples, contradicting existing research that presented a significant reduction in the abundance of SOX2-positive cells in the oSVZ of T21 brains ranging from PCW 12 to PCW 22[22]. However, this difference may be due to the limited number of biological replicates used in this study; here, two euploid and three T21 neocortex samples were used for immunofluorescence, whereas the other study quantifying the abundance of SOX2-positive cells used five euploid and six T21 neocortex samples[22], thereby improving the confidence with which a conclusion of reduced SOX2-positive cell abundance was reached. Regardless, it should be noted that when comparing the abundance of SOX2-positive radial glia at different gestational ages, it appears that SOX2-positive cells may be more abundant in T21 at PCW 13, but less abundant at PCW 17 and PCW 20, in comparison to age-matched euploids.

Various hypotheses exist regarding this potential reduction in neurogenic, SOX2-positive radial glia in T21. For instance, if radial glia do not proliferate as readily in the T21 neocortex compared to euploid tissue, the abundance of these cells may fail to increase[17]. Several results presented in this study relative to other studies are contradictory. For instance, the abundance of cells expressing PVIM, a mitotic cell marker, appeared to be greater in T21 at PCW 13, but lower at PCW 17 and PCW 20, with no significant difference between euploid and T21. Other studies using alternative cell proliferation markers, such as 5-ethynyl-2′-deoxyuridine (EdU) or antigen kiel 67 (Ki67), have demonstrated a reduction in cell proliferation in the fetal T21 neocortex[17,41]. This discrepancy may be attributed to various factors; for instance, the PVIM antibody used for immunofluorescence in this study showed a higher-than-ideal background in the VZ, which may have contributed to more quantification errors. Further, other studies have used different models of T21, such as mice[41,42], to demonstrate this reduction in cell proliferation. Ultimately, further studies using human tissue with an expanded sample size are imperative for understanding the effects of T21 on NPC proliferation; additional commercial PVIM antibodies or other mitotic markers, such as phospho-histone H3, could serve as alternatives.

Alternatively, radial glia may differentiate earlier in T21, thereby reducing the size of the NPC pool and abundance of these cells[17]. This explanation holds merit given the results of this study. Specifically, the abundance of SATB2-positive cells, differentiated callosally projecting neurons, appeared to be greater in the PCW 13 T21 neocortex in comparison to euploid tissue. However, this explanation is contested within existing literature, with some studies reporting delayed neuronal differentiation, while others

report earlier differentiation; regardless, the existence of a link between T21 and neuronal differentiation has been established[17,21,43,44]. These varying results may be driven by the various models used to demonstrate neuronal differentiation, such as fetal human tissue as opposed to mouse models, and highlights the need for further investigation into neuronal differentiation in T21[43,44].

Finally, radial glia may undergo increased apoptosis in the fetal T21 neocortex as compared to the euploid neocortex. Cultured NPCs from PCW 17 to PCW 19 T21 neocortices have been shown to exhibit increased expression of glial cell markers, such as *S100B,* in comparison to euploid, age-matched NPCs[38]. As mentioned above, elevated S100B expression may trigger increased production of reactive oxygen species, thereby driving NPC apoptosis[29,38]. A mouse model of T21 demonstrated no differences in the abundance of cells expressing cleaved caspase-3, an apoptosis marker, seemingly rejecting the hypothesis of increased NPC apoptosis[41]. However, given the genetic differences between mice and humans, further studies in primary human tissues are needed to confirm the generalizability of this observation before establishing a mechanistic cause of reduced SOX2-positive cell abundance in T21.

4.3. DACH1 and GPC6 may regulate early neurodevelopment and synaptogenesis

Interestingly, expression of downstream targets of GDF15, GPC6 and DACH1, qualitatively appeared to be lower at PCW 13 in T21 as compared to PCW 12 in euploid neocortices, and seemed to decrease, but not notably differ between euploid and T21 neocortices at PCW 16 to PCW 20. This observation was not corroborated by cell quantification comparing euploid oSVZs to T21 oSVZs, which showed no significant difference in DACH1-positive cell abundance, nor in *GPC6* and *DACH1* gene expression

between these neocortices, as shown by RT-qPCR data. With a larger sample size to compare gene expression and cellular abundance across gestational ages, greater *DACH1* expression at earlier rather than later gestational ages in euploid neocortices has been previously observed[45], potentially explaining the reduction in DACH1-positive cells from PCW 16 to PCW 20. In early neurogenesis, DACH1 has been shown to play an essential role in proper neural crest cell migration in *Xenopus laevis*, and has been found to later regulate the tactile sensitivity of somatosensory neurons in mice, but not their neurogenesis[46,47]. While these studies implicate DACH1 in early NPC development and differentiated neuron function in other species, respectively, the function of DACH1 in fetal human neurodevelopment is not yet known and warrants further investigation to understand the influence of the potential reduction of DACH1-positive cells on neurogenesis and intellectual disability in T21. Interestingly, *Gpc6* has been shown to modulate synaptogenesis and induce excitatory synapse formation in an *in vitro* model of rat neurogenesis, and is significantly associated with formal thought disorder – a manifestation of schizophrenia – in humans[48–50]. A hallmark of these disorders is a reduction in synapse abundance in adolescence and, presumably, during fetal neurodevelopment[50,51]. However, the role of GPC6 in synapse reduction in these disorders and T21 has not been studied; further studies on the role of GPC6 in synaptogenesis is worthwhile to expand our understanding of intellectual disability and other neurological conditions.

4.4. Elevated *SEMA5A* expression in T21 may alter axon guidance

This study demonstrated a significantly higher expression of the downstream GDF15 target, *SEMA5A*, in the developing T21 neocortex compared to euploid

neocortices. *SEMA5A* is first expressed in early embryogenesis, at PCW 8 to PCW 9, and functions as a bifunctional axon guidance cue, with attractant and repellent effects to guide developing axon migration[52,53]. Further, SEMA5A inhibits synaptogenesis and dendritic spine density in the granule cells, a specialized neuron type, of the hippocampus in newborn mice[54]. These phenotypes are observed in the newborn, but not embryonic, T21 neocortex[17]; altered axon guidance may result in disrupted synaptogenesis, and ultimately, altered formation of neural circuits, potentially leading to the intellectual disability observed in T21[17,55]. Interestingly, *SEMA5A* is expressed in various regions of the mature neocortex, including the primary somatosensory cortex, primary motor cortex, and areas of the temporal lobe; these regions are involved in sensory and motor skill acquisition – skills that are altered in individuals with T21[17,52,56].

Further, *SEMA5A* is an autism-susceptibility gene, and a reduction in its gene expression has been associated with increased risk of the disorder[52,53,57]. Interestingly, individuals with autism have an increase in synaptic density within their frontal, temporal, and parietal cortices[58]. Given the increased expression of *SEMA5A* in T21 presented here and the potential influence of SEMA5A on synaptogenesis in individuals with autism, it is reasonable to believe that increased SEMA5A in T21 may decrease synaptogenesis in these individuals. Analysis of synaptogenesis in the fetal T21 neocortex is essential to test this hypothesis, representing a research gap worth investigating.

In conclusion, this study highlights the potential role of T21 on neural and glial progenitor abundance via various GDF15 targets, demonstrating this pathway's contribution to certain phenotypes observed in T21 patients. To date, no other studies have identified a relationship between the GDF15 pathway and T21 neurodevelopment. With

this new understanding, clinicians can work with individuals with T21 to expand the scope of neurodevelopmental support programs for intellectual disability.

5. Literature Cited

1. Florio, M., and Huttner, W.B. (2014). Neural progenitors, neurogenesis and the evolution of the neocortex. Development *141*, 2182–2194. https://doi.org/10.1242/dev.090571.

2. Xing, L., Wilsch-Bräuninger, M., and Huttner, W.B. (2021). How neural stem cells contribute to neocortex development. Biochem Soc Trans *49*, 1997–2006. https://doi.org/10.1042/BST20200923.

3. Tabata, H. (2015). Diverse subtypes of astrocytes and their development during corticogenesis. Front Neurosci *9*. https://doi.org/10.3389/fnins.2015.00114.

4. Fletcher, J.L., Makowiecki, K., Cullen, C.L., and Young, K.M. (2021). Oligodendrogenesis and myelination regulate cortical development, plasticity and circuit function. Semin Cell Dev Biol *118*, 14–23. https://doi.org/10.1016/j.semcdb.2021.03.017.

5. Silbereis, J.C., Pochareddy, S., Zhu, Y., Li, M., and Sestan, N. (2016). The cellular and molecular landscapes of the developing human central nervous system. Neuron *89*, 248–268. https://doi.org/10.1016/j.neuron.2015.12.008.

6. Choi, B.H., Kim, R.C., and Lapham, L.W. (1983). Do radial glia give rise to both astroglial and oligodendroglial cells? Dev Brain Res *8*, 119–130. https://doi.org/10.1016/0165-3806(83)90163-3.

7. Kuhn, S., Gritti, L., Crooks, D., and Dombrowski, Y. (2019). Oligodendrocytes in development, myelin generation and beyond. Cells (2073-4409) *8*, 1424–1424. https://doi.org/10.3390/cells8111424.

8. Zhu, X., Bergles, D.E., and Nishiyama, A. (2008). NG2 cells generate both oligodendrocytes and gray matter astrocytes. Development *135*, 145–157. https://doi.org/10.1242/dev.004895.

9. Rogujski, P., Lukomska, B., Janowski, M., and Stanaszek, L. (2024). Glial-restricted progenitor cells: a cure for diseased brain? Biol Res *57*, 8. https://doi.org/10.1186/s40659-024-00486-1.

10. Iglesias, P., Silvestre, R.A., and Díez, J.J. (2023). Growth differentiation factor 15 (GDF-15) in endocrinology. Endocrine *81*, 419–431. https://doi.org/10.1007/s12020-023-03377-9.

11. Wang, D., Day, E.A., Townsend, L.K., Djordjevic, D., Jørgensen, S.B., and Steinberg, G.R. (2021). GDF15: emerging biology and therapeutic applications for obesity and cardiometabolic disease. Nat Rev Endocrinol *17*, 592–607. https://doi.org/10.1038/s41574-021-00529-7.

12. Carrillo-García, C., Prochnow, S., Simeonova, I.K., Strelau, J., Hölzl-Wenig, G., Mandl, C., Unsicker, K., von Bohlen und Halbach, O., and Ciccolini, F. (2014). Growth/differentiation factor 15 promotes EGFR signalling, and regulates proliferation and migration in the hippocampus of neonatal and young adult mice. Development *141*, 773–783. https://doi.org/10.1242/dev.096131.

13. Shin, H., Wong, E., Gohr, A., Ray, S., Morris, S., Mohamad, R., Derihaci, R., Wimberger, P., Strelau, J., Huttner, W., et al. Placenta-derived growth differentiation factor 15 promotes neural progenitor proliferation in the developing mammalian neocortex. Cell Reports (CELL-REPORTS-D-26-00043, in revision).

14. Kusre, G., Sarma, M., Nirmolia, T., and Shankarishan, P. (2015). Robertsonian translocation t (21; 21) in a female born to normal parents: a case report. J Clin Diagn Res *9*, gd01–gd02. https://doi.org/10.7860/jcdr/2015/10638.5372.

15. Antonarakis, S.E., Skotko, B.G., Rafii, M.S., Strydom, A., Pape, S.E., Bianchi, D.W., Sherman, S.L., and Reeves, R.H. (2020). Down syndrome. Nat Rev Dis Primers *6*, 9. https://doi.org/10.1038/s41572-019-0143-7.

16. Bull, M.J. (2020). Down syndrome. N Engl J Med *382*, 2344–2352. https://doi.org/10.1056/NEJMra1706537.

17. Russo, M.L., Sousa, A.M.M., and Bhattacharyya, A. (2024). Consequences of trisomy 21 for brain development in Down syndrome. Nat Rev Neurosci *25*, 740–755. https://doi.org/10.1038/s41583-024-00866-2.

18. Kondo, T., and Raff, M. (2000). Oligodendrocyte precursor cells reprogrammed to become multipotential CNS stem cells. Science *289*, 1754–1757. https://doi.org/10.1126/science.289.5485.1754.

19. Tanner, D.C., Cherry, J.D., and Mayer-Pröschel, M. (2011). Oligodendrocyte progenitors reversibly exit the cell cycle and give rise to astrocytes in response to

interferon-γ. J Neurosci *31*, 6235–6246. https://doi.org/10.1523/jneurosci.5905-10.2011.

20. Kanaumi, T., Milenkovic, I., Adle-Biassette, H., Aronica, E., and Kovacs, G.G. (2013). Non-neuronal cell responses differ between normal and Down syndrome developing brains. Int J Dev Neurosci *31*, 796–803. https://doi.org/10.1016/j.ijdevneu.2013.09.011.

21. Chakrabarti, L., Galdzicki, Z., and Haydar, T.F. (2007). Defects in embryonic neurogenesis and initial synapse formation in the forebrain of the Ts65Dn mouse model of Down syndrome. J Neurosci *27*, 11483–11495. https://doi.org/10.1523/jneurosci.3406-07.2007.

22. Baburamani, A.A., Vontell, R.T., Uus, A., Pietsch, M., Patkee, P.A., Wyatt-Ashmead, J., Chin-Smith, E.C., Supramaniam, V.G., Donald Tournier, J., Deprez, M., et al. (2020). Assessment of radial glia in the frontal lobe of fetuses with Down syndrome. Acta Neuropathol Commun *8*, 141. https://doi.org/10.1186/s40478-020-01015-3.

23. Mohamad, R. (2025). Regulation of gene expression by growth differentiation factor 15 in the developing mouse and human neocortex. Honours Thesis. The University of Manitoba, pp. 9, 19-20. https://doi.org/hdl.handle.net/1993/39089.

24. Hansen, D.V., Lui, J.H., Parker, P.R.L., and Kriegstein, A.R. (2010). Neurogenic radial glia in the outer subventricular zone of human neocortex. Nature *464*, 554–561. https://doi.org/10.1038/nature08845.

25. Holst, C.B., Brøchner, C.B., Vitting-Seerup, K., and Møllgård, K. (2023). The HOPX and BLBP landscape and gliogenic regions in developing human brain. J Anat *243*, 23–38. https://doi.org/10.1111/joa.13844.

26. Alcamo, E.A., Chirivella, L., Dautzenberg, M., Dobreva, G., Fariñas, I., Grosschedl, R., and McConnell, S.K. (2008). Satb2 regulates callosal projection neuron identity in the developing cerebral cortex. Neuron *57*, 364–377. https://doi.org/10.1016/j.neuron.2007.12.012.

27. Reillo, I., De Juan Romero, C., García-Cabezas, M.Á., and Borrell, V. (2011). A role for intermediate radial glia in the tangential expansion of the mammalian cerebral cortex. Cereb Cortex *21*, 1674–1694. https://doi.org/10.1093/cercor/bhq238.

28. Szu, J., Wojcinski, A., Jiang, P., and Kesari, S. (2021). Impact of the Olig family on neurodevelopmental disorders. Front Neurosci *15, 659601*. https://doi.org/10.3389/fnins.2021.659601.

29. Hernández-Ortega, K., Canul-Euan, A.A., Solis-Paredes, J.M., Borboa-Olivares, H., Reyes-Muñoz, E., Estrada-Gutierrez, G., and Camacho-Arroyo, I. (2024). S100B actions on glial and neuronal cells in the developing brain: an overview. Front Neurosci *18, 1425525*. https://doi.org/10.3389/fnins.2024.1425525.

30. Chakrabarti, L., Best, T.K., Cramer, N.P., Carney, R.S.E., Isaac, J.T.R., Galdzicki, Z., and Haydar, T.F. (2010). Olig1 and Olig2 triplication causes developmental brain defects in Down syndrome. Nat Neurosci *13*, 927–934. https://doi.org/10.1038/nn.2600.

31. Xing, L., Kalebic, N., Namba, T., Vaid, S., Wimberger, P., and Huttner, W.B. (2020). Serotonin receptor 2A activation promotes evolutionarily relevant basal progenitor proliferation in the developing neocortex. Neuron *108*, 1113-1129.e6. https://doi.org/10.1016/j.neuron.2020.09.034.

32. Schindelin, J., Arganda-Carreras, I., Frise, E., Kaynig, V., Longair, M., Pietzsch, T., Preibisch, S., Rueden, C., Saalfeld, S., Schmid, B., et al. (2012). Fiji: an open-source platform for biological-image analysis. Nat Methods *9*, 676–682. https://doi.org/10.1038/nmeth.2019.

33. Tarnowski, B.I., Spinale, F.G., and Nicholson, J.H. (1991). DAPI as a useful stain for nuclear quantitation. Biotech Histochem *66*, 297–302.

34. Lu, J., Esposito, G., Scuderi, C., Steardo, L., Delli-Bovi, L.C., Hecht, J.L., Dickinson, B.C., Chang, C.J., Mori, T., and Sheen, V. (2011). S100B and APP promote a gliocentric shift and impaired neurogenesis in Down syndrome neural progenitors. PLoS One *6*, e22126. https://doi.org/10.1371/journal.pone.0022126.

35. Lu, J., Lian, G., Zhou, H., Esposito, G., Steardo, L., Delli-Bovi, L.C., Hecht, J.L., Lu, Q.R., and Sheen, V. (2012). OLIG2 over-expression impairs proliferation of human Down syndrome neural progenitors. Hum Mol Genet *21*, 2330–2340. https://doi.org/10.1093/hmg/dds052.

36. Griffin, W.S., Stanley, L.C., Ling, C., White, L., MacLeod, V., Perrot, L.J., White, C.L., and Araoz, C. (1989). Brain interleukin 1 and S-100 immunoreactivity are

elevated in Down syndrome and Alzheimer disease. Proc Natl Acad Sci U-S-A *86*, 7611–7615. https://doi.org/10.1073/pnas.86.19.7611.

37. Sheng, J.G., Mrak, R.E., Bales, K.R., Cordell, B., Paul, S.M., Jones, R.A., Woodward, S., Zhou, X.Q., McGinness, J.M., and Griffin, W.S.T. (2000). Overexpression of the neuritotrophic cytokine S100β precedes the appearance of neuritic β-amyloid plaques in APPV717F mice. J Neurochem *74*, 295–301. https://doi.org/10.1046/j.1471-4159.2000.0740295.x.

38. Esposito, G., Imitola, J., Lu, J., De Filippis, D., Scuderi, C., Ganesh, V.S., Folkerth, R., Hecht, J., Shin, S., Iuvone, T., et al. (2008). Genomic and functional profiling of human Down syndrome neural progenitors implicates S100B and aquaporin 4 in cell injury. Hum Mol Genet *17*, 440–457. https://doi.org/10.1093/hmg/ddm322.

39. Jiang, W., Chen, L., and Zheng, S. (2021). Global reprogramming of apoptosis-related genes during brain development. Cells *10*, 2901. https://doi.org/10.3390/cells10112901.

40. Rueda, N., Flórez, J., and Martínez-Cué, C. (2013). Apoptosis in Down's syndrome: lessons from studies of human and mouse models. Apoptosis *18*, 121–134. https://doi.org/10.1007/s10495-012-0785-3.

41. Kurabayashi, N., Fujii, K., Otobe, Y., Hiroki, S., Hiratsuka, M., Yoshitane, H., Kazuki, Y., and Takao, K. (2023). Neocortical neuronal production and maturation defects in the TcMAC21 mouse model of Down syndrome. iScience *26, 12*. https://doi.org/10.1016/j.isci.2023.108379.

42. Contestabile, A., Fila, T., Ceccarelli, C., Bonasoni, P., Bonapace, L., Santini, D., Bartesaghi, R., and Ciani, E. (2007). Cell cycle alteration and decreased cell proliferation in the hippocampal dentate gyrus and in the neocortical germinal matrix of fetuses with down syndrome and in Ts65Dn mice. Hippocampus *17*, 665–678. https://doi.org/10.1002/hipo.20308.

43. Olmos-Serrano, J.L., Kang, H.J., Tyler, W.A., Silbereis, J.C., Cheng, F., Zhu, Y., Pletikos, M., Jankovic-Rapan, L., Cramer, N.P., Galdzicki, Z., et al. (2016). Down syndrome developmental brain transcriptome reveals defective oligodendrocyte differentiation and myelination. Neuron *89*, 1208–1222. https://doi.org/10.1016/j.neuron.2016.01.042.

44. Lattke, M., Tan, W.L., Sukumaran, S.K., Utami, K.H., Sintes, M., Sakthivel, S., Tan, J., Lim, A., Bansal, V.A., Rekopoulou, K., et al. (2026). Single-cell atlas of the developing Down syndrome brain cortex. Nat Med, 1–12. https://doi.org/10.1038/s41591-026-04211-1.

45. Castiglioni, V., Faedo, A., Onorati, M., Bocchi, V.D., Li, Z., Iennaco, R., Vuono, R., Bulfamante, G.P., Muzio, L., Martino, G., et al. (2019). Dynamic and cell-specific DACH1 expression in human neocortical and striatal development. Cereb Cortex *29*, 2115–2124. https://doi.org/10.1093/cercor/bhy092.

46. Szemes, T., Sabaté San José, A., Azouz, A., Sitte, M., Salinas, G., Achouri, Y., Kricha, S., Ris, L., Red-Horse, K., Bellefroid, E.J., et al. (2025). Temporal refinement of Dach1 expression contributes to the development of somatosensory neurons. EMBO J *44*, 2882–2905. https://doi.org/10.1038/s44318-025-00427-y.

47. Kim, Y.-K., Lee, H., Ismail, T., Kim, Y., and Lee, H.-S. (2020). Dach1 regulates neural crest migration during embryonic development. Biochem Biophys Res Commun *527*, 896–901. https://doi.org/10.1016/j.bbrc.2020.05.009.

48. Allen, N.J., Bennett, M.L., Foo, L.C., Wang, G.X., Chakraborty, C., Smith, S.J., and Barres, B.A. (2012). Astrocyte glypicans 4 and 6 promote formation of excitatory synapses via GluA1 AMPA receptors. Nature *486*, 410–414. https://doi.org/10.1038/nature11059.

49. Wang, K.-S., Zhang, Q., Liu, X., Wu, L., and Zeng, M. (2012). PKNOX2 is associated with formal thought disorder in schizophrenia: a meta-analysis of two genome-wide association studies. J Mol Neurosci *48*, 265–272. https://doi.org/10.1007/s12031-012-9787-4.

50. Kircher, T., Bröhl, H., Meier, F., and Engelen, J. (2018). Formal thought disorders: from phenomenology to neurobiology. Lancet Psychiatry *5*, 515–526. https://doi.org/10.1016/S2215-0366(18)30059-2.

51. Schmitt, A., Falkai, P., and Papiol, S. (2023). Neurodevelopmental disturbances in schizophrenia: evidence from genetic and environmental factors. J Neural Transm (Vienna) *130*, 195–205. https://doi.org/10.1007/s00702-022-02567-5.

52. Wang, Q., Liu, Z., Lin, Z., Zhang, R., Lu, Y., Su, W., Li, F., Xu, X., Tu, M., Lou, Y., et al. (2019). De novo germline mutations in SEMA5A associated with infantile spasms. Front Genet *10*, 605. https://doi.org/10.3389/fgene.2019.00605.

53. Nagy, G.N., Zhao, X.-F., Karlsson, R., Wang, K., Duman, R., Harlos, K., El Omari, K., Wagner, A., Clausen, H., Miller, R.L., et al. (2024). Structure and function of Semaphorin-5A glycosaminoglycan interactions. Nat Commun *15*, 2723. https://doi.org/10.1038/s41467-024-46725-7.

54. Duan, Y., Wang, S.-H., Song, J., Mironova, Y., Ming, G., Kolodkin, A.L., and Giger, R.J. (2014). Semaphorin 5A inhibits synaptogenesis in early postnatal- and adult-born hippocampal dentate granule cells. eLife *3*, e04390. https://doi.org/10.7554/eLife.04390.

55. Chen, S.-Y., and Cheng, H.-J. (2009). Functions of axon guidance molecules in synapse formation. Curr Opin Neurobiol *19*, 471–478. https://doi.org/10.1016/j.conb.2009.09.005.

56. Meejang, J., Busboom, M.T., Baker, S.E., Arif, Y., Kastner, O., Wilson, T.W., and Kurz, M.J. (2025). Adults with Down syndrome exhibit altered somatosensory cortical inhibition. Neuroimage Clin *46*, 103797. https://doi.org/10.1016/j.nicl.2025.103797.

57. Melin, M., Carlsson, B., Anckarsäter, H., Rastam, M., Betancur, C., Isaksson, A., Gillberg, C., and Dahl, N. (2006). Constitutional downregulation of SEMA5A expression in autism. Neuropsychobiology *54*, 64–69. https://doi.org/10.1159/000096040.

58. Tang, G., Gudsnuk, K., Kuo, S.-H., Cotrina, M.L., Rosoklija, G., Sosunov, A., Sonders, M.S., Kanter, E., Castagna, C., Yamamoto, A., et al. (2014). Loss of mTOR-

dependent macroautophagy causes autistic-like synaptic pruning deficits. Neuron *83*, 1131–1143. https://doi.org/10.1016/j.neuron.2014.07.040.